

PAPER • OPEN ACCESS

## Power Flux in Cylindrical Waveguide with Metamaterials

To cite this article: Sukaina Tuama Ghafel *et al* 2020 *IOP Conf. Ser.: Mater. Sci. Eng.* **928** 072158

View the [article online](#) for updates and enhancements.

You may also like

- [Density bunch formation by microwave in a plasma-filled cylindrical waveguide](#)  
Hitendra K. Malik
- [Nano-height cylindrical waveguide in GaN-based vertical-cavity surface-emitting lasers](#)  
Masaru Kuramoto, Seiichiro Kobayashi, Takanobu Akagi et al.
- [Cerenkov radiation in a cylindrical waveguide with elliptic cross section](#)  
R M Khan



**ECS**  
The  
Electrochemical  
Society  
Advancing solid state &  
electrochemical science & technology

**DISCOVER**  
how sustainability  
intersects with  
electrochemistry & solid  
state science research

## Power Flux in Cylindrical Waveguide with Metamaterials

Sukaina Tuama Ghafel, Hassan Abid Yasser, Abdul-Kareem Mahdi salih (\*)

(\*)Thi-Qar University, College of science, physics department.

E-mail: [tuamasukaina8@gmail.com](mailto:tuamasukaina8@gmail.com)

[hassan.yasserph@sci.utq.edu.iq](mailto:hassan.yasserph@sci.utq.edu.iq)

[abdulkareem@utq.edu.iq](mailto:abdulkareem@utq.edu.iq)

### Abstract—

Analytical and numerical analysis of electromagnetic wave propagation in cylindrical waveguides filled with isotropic metamaterial is presented. Emphasis is given to the characteristics of power flux in the waveguide. In the structure of the waveguide, The characteristics equation for the modes in this waveguide is obtained. The behavior of the dispersion curves and the energy flux are examined theoretically. The negative energy flux propagation through the cylindrical waveguide is confirmed.

*Keywords-cylindrical waveguide; Dispersion relation; isotropic metamaterial;SNG material; power flux.*

### 1. INTRODUCTION

Since the realization of negative refraction[1] in microwaves [2], there is renewed and intense interest in electromagnetic metamaterials. Negative refraction has added a new area to physics, leading to new concepts such as perfect lens [3], [4], superlens [5], and focusing by plano-concave lens [6]. Negative refraction has subsequently been realized in microwaves [7], THz waves, and optical wavelengths [8], in metamaterials made of wire and split-ring resonators [9] or photonic crystals[10]Metamaterials are artificial media composed of elements which dimension are small compared to the wavelength of interest. Metamaterials may display properties which are more noticeable than those observed in natural materials[11,12]. The famous example of these properties are metamaterials with a negative refractive index which are well known as negative index metamaterials (NIMs)[13,14,15], also called left handed materials (LHMs)[16,17].

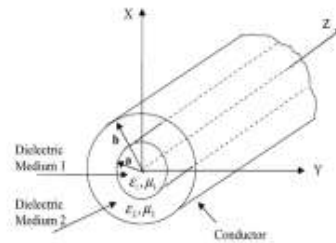
In this paper, investigate analysis and computations of the propagation of electromagnetic fields and energy flux density in the cylindrical waveguide structure with its core and cladding filled with single negative material. to purpose the new sign varying energy flux and their cancellation. We proved that the propagation of electromagnetic waves can stopped in the appropriate condition owing to the cancellation. The dispersion relations for the guide are derived and used to obtain the propagating modes, filled distribution and their power flux. Results that the frequency have factual effects on the power values of the propagating modes.



The MATLAB environment was adopted to solve the important equations, and because there are some theoretical approximations, we decided to design the same model in the COMSOL software and carry out the solutions by finite element method (FEM), and then compare the solutions of the two methods.

## 2. STRUCTURE OF DIELECTRIC CYLINDRICAL WAVEGUIDE FILLED WITH METAMATERIAL

In the presented model, dielectric cylindrical waveguide considered for electromagnetic wave modal characteristics study[18]. It has three regions as shown in Fig.(1). Inner core region is single negative medium having radius ( $0 < r < r_1$ ) and permittivity  $\epsilon_1$ . Second region is dielectric having radius ( $r_1 < r < r_2$ ) and permittivity  $\epsilon_2$ . Outer most region ( $r \rightarrow \infty$ ) is free space region extending up to infinity having permittivity  $\epsilon_3$ .



Fig(1):metamaterial cylindrical waveguide[19].

## 3. CHARACTERISTIC EQUATIONS

### A. Analytical theory

Consider cylinder coordinate system ( $\rho, \phi, z$ ), where  $z$  is axial wave propagation direction. The axial components of magnetic and electric field in each region can be expressed:

$$H_{z1} = A B_v^{m1}(k_{r1}r) \cos(v\phi) \exp(-jk_z z) \quad (1a)$$

$$E_{z1} = B B_v^{e1}(k_{r1}r) \sin(v\phi) \exp(-jk_z z) \quad (1b)$$

$$H_{z2} = A B_v^{m2}(k_{r2}r) \cos(v\phi) \exp(-jk_z z) \quad (2a)$$

$$E_{z2} = B B_v^{e2}(k_{r2}r) \sin(v\phi) \exp(-jk_z z) \quad (2b)$$

where  $A, B, C,$  and  $D$  are unknown constants that will be determined later. The functions  $B_v^{pq}(k_{r,q}r)$  denotes the radial variation of the fields with  $q = 1$  in core and  $q = 2$  in clad that are solutions to Bessel's equation of order  $v$ . The superscript  $p$  is either  $m$  for magnetic field or  $e$  for electric field, respectively. Propagation vectors are given as :

$$k_{r1}^2 = n_1^2 k^2 - k_z^2 \quad (3)$$

$$k_{r2}^2 = n_2^2 k^2 - k_z^2 \quad (4)$$

and  $n_1, n_2$  are the refractive indices of core and cladding, respectively.

### B. Boundary conditions and dispersion relation

For the present circular waveguide, the field must be finite at  $r = a$ ; hence

$$B_v^{m1}(k_{r1}r) = B_v^{e1}(k_{r1}r) = J_n(k_{r1}r) \quad (5)$$

To satisfy  $E_z = 0$  at  $r = b$ , we choose

$$B_v^{m2}(k_{r1}r) = J_n(k_{r2}r) Y_n(k_{r2}b) - J_n(k_{r2}b) Y_n(k_{r2}r) \quad (6)$$

Furthermore, to satisfy  $E_\varphi = 0$  at  $r = b$ , we choose

$$B_v^{e2}(k_{r1}r) = J_n(k_{r2}r) Y'_n(k_{r2}b) - J'_n(k_{r2}b) Y_n(k_{r2}r) \quad (7)$$

Expressing the tangential field components ( $E_r, E_\varphi, H_r$  and  $H_\varphi$ ) as functions of the longitudinal field components ( $E_z$  and  $H_z$ ), yield

$$ik_z E_\varphi - i\omega\mu_0\mu H_r = \frac{1}{r} \frac{\partial E_z}{\partial \varphi} \quad (8a)$$

$$-ik_z E_r + i\omega\mu_0\mu H_\varphi = \frac{\partial E_z}{\partial r} \quad (8b)$$

$$i\omega\varepsilon\varepsilon_0 E_r - ik_z H_\varphi = \frac{1}{r} \frac{\partial H_z}{\partial \varphi} \quad (8c)$$

$$i\omega\varepsilon\varepsilon_0 E_\varphi + ik_z H_r = -\frac{\partial H_z}{\partial r} \quad (8d)$$

Using the above equations, the radial and azimuthal fields components inside core and clad regions will be

$$E_{ri} = \frac{i\omega\mu_0\mu_i}{k_{ri}^2} \left( \frac{k_z}{\omega\mu_0\mu_i} \frac{\partial E_{zi}}{\partial r} + \frac{1}{r} \frac{\partial H_{zi}}{\partial \varphi} \right) \quad (9a)$$

$$E_{\varphi i} = \frac{i\omega\mu_0\mu_i}{k_{ri}^2} \left( \frac{k_z}{\omega\mu_0\mu_i} \frac{1}{r} \frac{\partial E_{zi}}{\partial \varphi} - \frac{\partial H_{zi}}{\partial r} \right) \quad (9b)$$

$$H_{ri} = \frac{ik_z}{k_{ri}^2} \left( \frac{\partial H_{zi}}{\partial r} - \frac{\omega\varepsilon_0\varepsilon_i}{k_z} \frac{1}{r} \frac{\partial E_{zi}}{\partial \varphi} \right) \quad (9c)$$

$$H_{\varphi i} = -\frac{ik_z}{k_{ri}^2} \left( \frac{\omega\varepsilon_0\varepsilon_i}{k_z} \frac{\partial E_{zi}}{\partial r} + \frac{1}{r} \frac{\partial H_{zi}}{\partial \varphi} \right) \quad (9d)$$

where  $i = 1, 2$  for core and clad, respectively.

Applying the boundary conditions to the tangential field components i.e.,  $z$  and  $\varphi$  components, at  $\rho = a$ . Using all components  $4 \times 4$  coefficient matrix is constructed and the characteristic equation is derived (see [19]). From the condition that the determinant of the matrix should be zero, the characteristic relation and field distribution of the cylindrical waveguide can be obtained as,

$$\left( \frac{\varepsilon_1}{\varepsilon_2} |k_{r2}| \frac{\Lambda'_1}{\Lambda_1} - |k_{r1}| \frac{\Lambda'_3}{\Lambda_3} \right) \left( \frac{\mu_1}{\mu_2} |k_{r2}| \frac{\Lambda'_1}{\Lambda_1} - |k_{r1}| \frac{\Lambda'_4}{\Lambda_4} \right) = \frac{v^2 k_z^2}{k_0^2 a^2} \frac{(k_{r2}^2 - k_{r1}^2)^2}{k_{r1}^2 k_{r2}^2} \quad (10)$$

where the parameters  $\Lambda'_i, \Lambda_i$  are defined as

$$\Lambda_1 = \Lambda_2 = iI_1(|k_{r1}|a) \quad (11a)$$

$$\Lambda'_1 = \Lambda'_2 = iI'_1(|k_{r1}|a) \quad (11b)$$

$$\Lambda_3 = \frac{2}{\pi} [K_1(|k_{r2}|a)I_1(|k_{r2}|b) - K_1(|k_{r2}|b)I_1(|k_{r2}|a)] \quad (11c)$$

$$\Lambda'_3 = \frac{2}{\pi} \left[ \frac{1}{|k_{r2}|a} \{K_1(|k_{r2}|a)I_1(|k_{r2}|b) - K_1(|k_{r2}|b)I_1(|k_{r2}|a)\} \right. \\ \left. - \{I_1(|k_{r2}|b)K_2(|k_{r2}|a) + I_2(|k_{r2}|a)K_1(|k_{r2}|b)\} \right] \quad (11d)$$

$$\Lambda_4 = \frac{2}{\pi} \left[ K_1(|k_{r2}|a) \left( \frac{1}{|k_{r2}|b} I_1(|k_{r2}|b) + I_2(|k_{r2}|b) \right) - \right. \\ \left. I_1(k_{r2}a) \left( \frac{1}{|k_{r2}|b} K_1(|k_{r2}|b) - K_2(|k_{r2}|b) \right) \right] \quad (11e)$$

### C. Fields and Power Flux

In this section, the field expressions will be determined, which will be used to construct the power flux that refers the type of propagation, computing the constants  $A, B, C, D$  and Substituting these constants into Eqs.(1) and (2), the fields distributions in the core and clad will be

$$H_{z1} = A J_v(k_{r1}r) \cos(v\phi) e^{-jk_z z} \quad (12a)$$

$$E_{z1} = B J_v(k_{r1}r) \sin(v\phi) e^{-jk_z z} \quad (12b)$$

$$H_{z2} = C \begin{bmatrix} J_v(k_{r2}r) Y_v(k_{r2}b) \\ -J_v(k_{r2}b) Y_v(k_{r2}r) \end{bmatrix} \cos(v\phi) e^{-jk_z z} \quad (12c)$$

$$E_{z2} = D \begin{bmatrix} J_v(k_{r2}r) Y'_v(k_{r2}b) \\ -J'_v(k_{r2}b) Y_v(k_{r2}r) \end{bmatrix} \sin(v\phi) e^{-jk_z z} \quad (12d)$$

The final field formulas by which the distribution of the various achieved modes within the waveguide can be drawn. The electric/magnetic power is defined as [12]

$$P_i^{TE} = \frac{k_z}{2\omega \mu_1} \int_0^a \int_0^{2\pi} |E_{z1}|^2 r dr d\phi + \frac{k_z}{2\omega \mu_2} \int_a^b \int_0^{2\pi} |E_{z2}|^2 r dr d\phi \quad (13)$$

$$P_i^{TM} = \frac{k_z}{2\omega \epsilon_1} \int_0^a \int_0^{2\pi} |H_{z1}|^2 r dr d\phi + \frac{k_z}{2\omega \epsilon_2} \int_a^b \int_0^{2\pi} |H_{z2}|^2 r dr d\phi \quad (14)$$

where  $i=1,2$  represents the layer index,  $P_i^{TE} / P_i^{TM}$  are the electric/magnetic power in the layer  $i$  for each mode in the waveguide. The electric/magnetic power in the individual layers may be done by substituting Eqs.(12a) and Eqs. (12c) into Eqs.(13), and evaluating the definite integrals numerically. The total normalized power (power flux) carried by each mode in the z-direction takes the form [15]

$$\bar{P} = \frac{P_1^\alpha + P_2^\alpha}{|P_1^\alpha| + |P_2^\alpha|} \quad (15)$$

where  $\alpha = TE, TM$ . When  $\bar{P} < 0$ , the net total power flow of the guided mode is antiparallel the direction of phase flow and this wave is called backward wave. One can get the opposite result when  $\bar{P} > 0$  and this wave is called the forward wave. While at  $\bar{P} = 0$ , the wave is stopped. It is important to note that the value of  $\bar{P}$  depends on the operation parameters such frequency, effective refractive index, and the radii of the core and clad.

#### 4. RESULT DISSECTION

The guided modal properties of cylindrical waveguides can be analyzed in terms of their dispersion curves, i.e. effective refractive index versus frequency, which are solutions of the characteristic equation outlined in the previous section. First, the modal behavior of SNG cylindrical waveguides is investigated with several combinations of simultaneously positive dielectric and magnetic constants. The work focus on the mode properties and electric field distribution, however the modes properties simulated using Eqs.( 10) the field distributions are presented using Eqs.(12a.12b.12c) and (12d). The theoretical program depends on dividing  $w, n_{eff}$  into very accurate intervals to ensure the accuracy of the results but that causes too much time loss by the computer, so we thought to balance the accuracy of the results and achieve an acceptable time for calculations. Note that the increased repetition causes increased amputation and recycling errors .

COMSOL program depends on the system solution numerically in a way FEM and relies on the division of the period to the greater number of triangles has increased the time of calculation and may cause a significant increase program stops. However, our simulation is characterized by many different parameters. There are another parameters that will be changed through simulation depending on the mode order and the normalized frequency. Note that, the simulations depends on permittivity and permeability.

The material of  $\epsilon, \mu$  has different signal does not propagation, but the synthesis of two materials of  $\epsilon, \mu$  inside are (-,+ ) and outside (+,-) led to the achievement of waveguide. Solve the characteristic equation with complex numbers is difficult and needs very much time so we cut it solved on the real part only .

##### 4.1 Permittivity and Permeability

**Figure(1)** represents the relation of  $\epsilon_1, \mu_2$  as a function of the frequency in the left figure, in the middle figure the relation of the imaginary part of  $n_{clad}, n_{core}$  with the frequency, while the right figure indicates the relation of the real part of  $n_{clad}, n_{core}$  with the frequency. We want  $\epsilon_1, \mu_2 < 0$  to be achieved within the range (1.8-5) GHz. This range can be changed according to  $w_{pe}, w_{pm}$ , which is related to the geometry of the studied media. In the range (5-7.2)GHz, we have different signs of  $\epsilon_1, \mu_2$ . The range beyond 7.2GHz represents positive values for both factors  $\epsilon_1, \mu_2$ . In the range (1.8-5) GHz, you can note that  $n_{clad}, n_{core}$  are pure imaginary with  $n_{clad} < n_{core}$ . At some frequencies,  $\epsilon_1, \mu_2$  will be zero, so the refractive index is zero, and this causes complex physical phenomena outside the subject of our study. We also note that after the frequency values that make the refractive index zero, we will get a positive refractive index and this represents normal materials. Within the chosen frequency range, the refractive indices are imaginary, and this means that there is no propagation at each individual

material. It will become evident later that the synthesis of these two materials within the waveguide leads to the possibility of achieving complex indices and this allows modes to propagation.

#### 4.2 Modes in Normal Cylindrical Waveguide

**Figure(2)** explains the dispersion relation of modes in a normal cylindrical waveguide, where the modes indicated in the figure. As it indicates, the normalized frequency is  $V = k_0 a \sqrt{n_{core}^2 - n_{clad}^2}$ . An ordinary cylindrical waveguide means optical fiber consisting of ordinary materials in which  $\epsilon_1, \epsilon_2, \mu_2, \mu_1$  are all positive. It becomes evident here that all curves increase with increasing frequency until they reach a certain value. This means that all modes have a forward propagation through the waveguide. On the other hand, the fundamental mode  $LP_{01}$  is the first to appear with increasing the normalized frequency, and the cut-off frequency for a single mode waveguide is  $V = 2.405$ . As  $V$  increases, the higher modes begin to appear, and it must be noted here for each mode there is a different propagation way that determined by the relation depicted in the figure.

**Figure(3)** represents the dispersion curves for the modes  $LP_{01}, LP_{11}, LP_{12}, LP_{21}$  and  $LP_{22}$  for cylindrical waveguides with metamaterial. Where the left side indicates the analytical results and the right side indicates the numerical results, and the different colors indicate the radius of the core ( $a = 10, 12, 14$ )  $\mu\text{m}$ . At the beginning, we note the matching of the two methods in the case of the fundamental mode  $LP_{01}$  and that the curve will decrease with increasing radius and this is physically acceptable as an increasing of radius leads to greater ability of fields to propagation through the core. In the case of other modes, we see that the analytical and numerical method agree in some parts of the modes and differ in others. Generally we see that the curves decrease in some locations with increasing radius. It is also noted that all curves raise at (5 GHz). That is; we approach the zero value of one of the refractive index.

The figures of dispersion here are complex and do not similar to a normal cylindrical waveguide. The constructed complexity here will cause a strange propagation of the mode, either forward or backward. Sometimes, modes with higher  $n_{eff}$  are referred to as slow modes such as  $LP_{22}, LP_{12}$ , and modes with lower  $n_{eff}$  are as fast modes such as  $LP_{11}$  and  $LP_{21}$ . We cannot confirm here which of the two methods is the closest to reality, since the analytical method dependent certain approximations and the numerical method also causes errors in relation to the selected mesh accuracy and the truncation errors.

#### 4.3 Power Flux

**Fig.(4)** represents the power flux as a function of frequency for modes  $LP_{01}, LP_{11}, LP_{12}, LP_{21}, LP_{22}$ . It is evident from the figure that all modes start with a backward propagation, after which the curve increases to be zero power flux at a certain frequency and then the forward propagation of positive power flux will happen. The fact “zero power flux” means the stopping light. It is also evident from the figure that the extent of the forward and backward propagations of all modes are different. In general, the fundamental mode achieves stopping light at the lowest frequency compared to other modes. The high order modes are not subject to a fixed sequence to achieve the stopping light and this is due to the nature of the dispersion relation for each mode.

**Fig.(5)** represents the power flux of the fundamental mode using different values for the radius of the core ( $a = 8, 10, 11$ )  $\mu\text{m}$ . Smaller radius achieves a stopping light at a lower frequency. Generally, when moving away from the stopping light point, the behavior of the power flux with frequency does not differ much with changing core radius. Figs.(3) and (4)

represent the total behavior of the mode power with change the frequency. Generally, increasing frequency will make propagation forward.

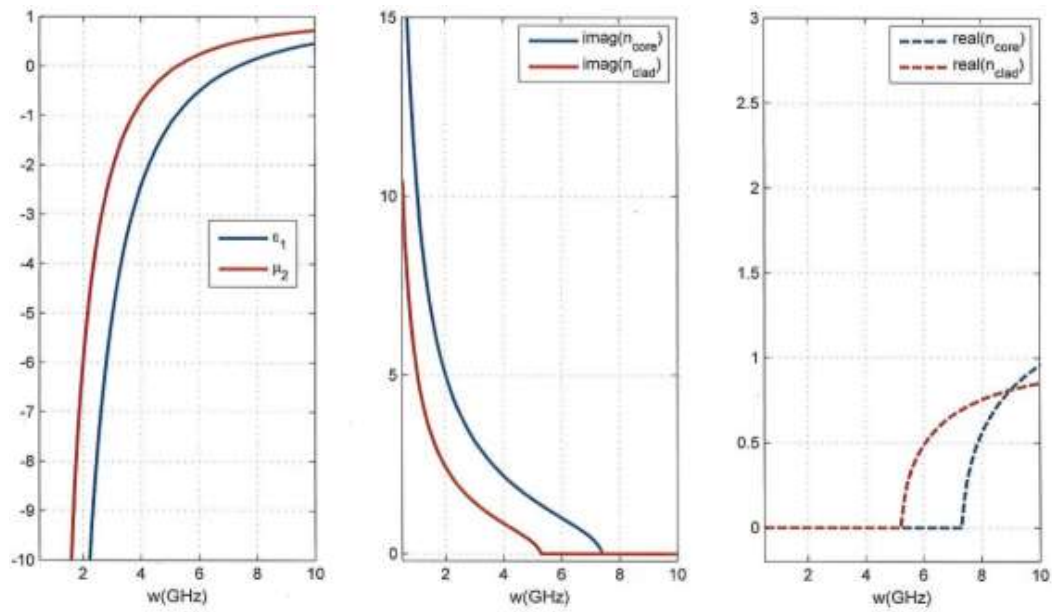


**Fig.(1):** permittivity, permeability and refractive indices as a function of frequency.

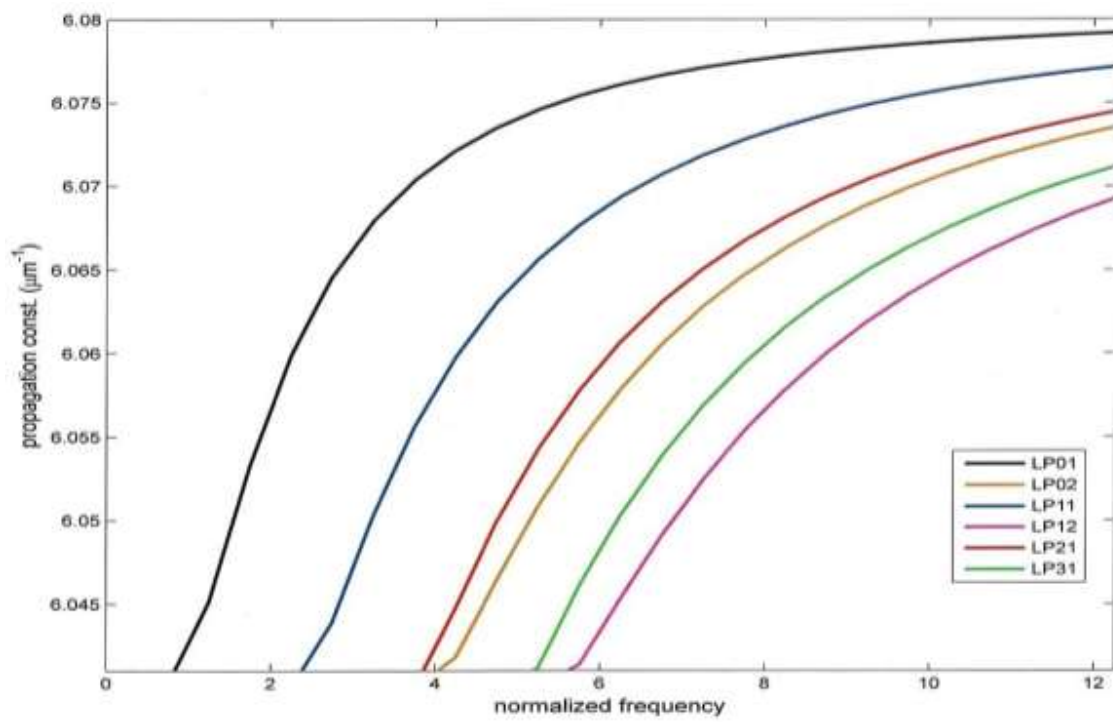
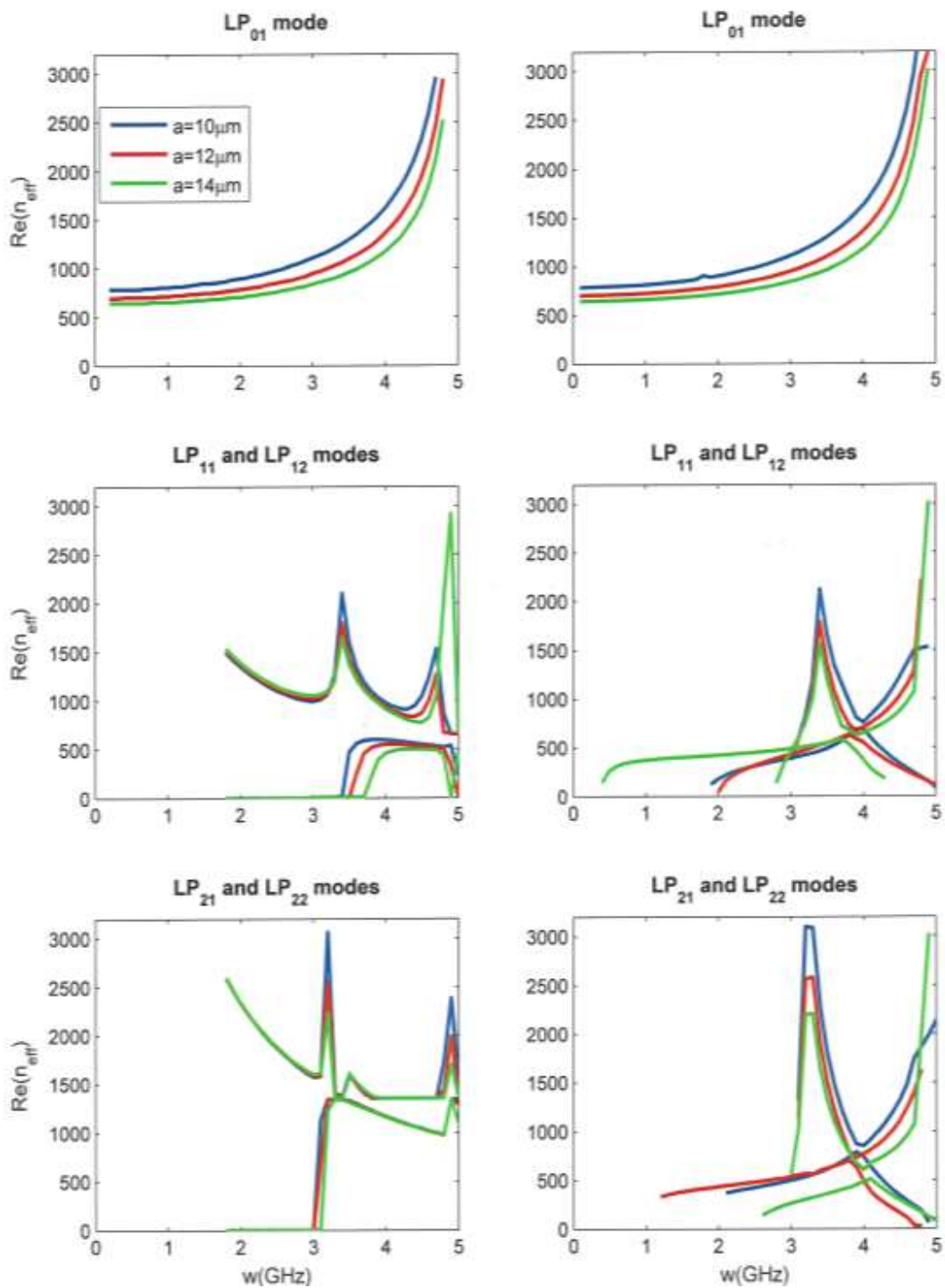
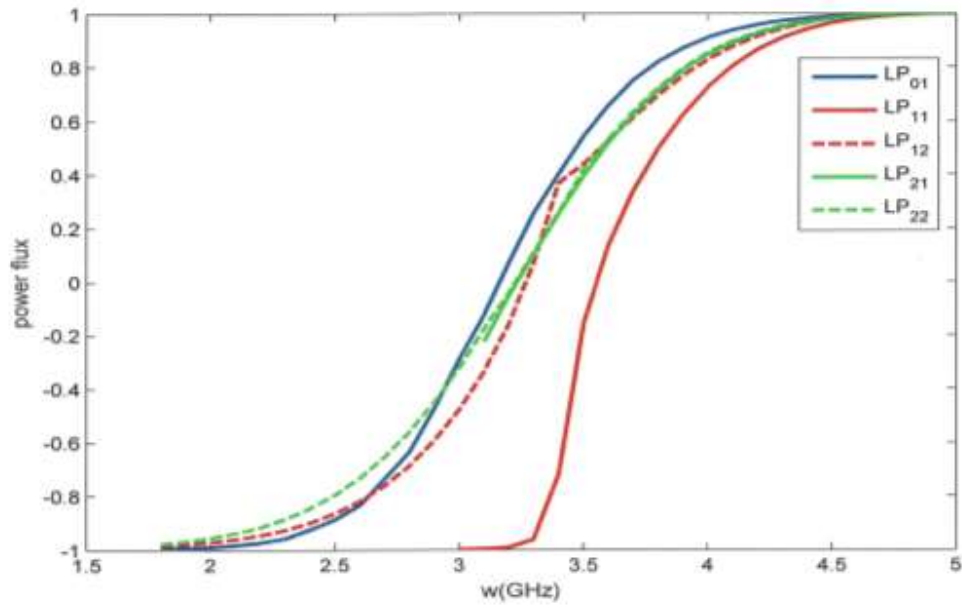


Fig.(2): dispersion relation in normal cylindrical waveguide.



**Fig.(3):** dispersion relation of the modes  $LP_{01}, LP_{11}, LP_{12}, LP_{21}, LP_{22}$  in cylindrical waveguide with SNG metamaterial, where the left column represents the analytical results, while the right column represents the FEM results.



**Fig.(4):** electrical power flux as a function of frequency  
for  $LP_{01}, LP_{11}, LP_{12}, LP_{21}, LP_{22}$  modes.

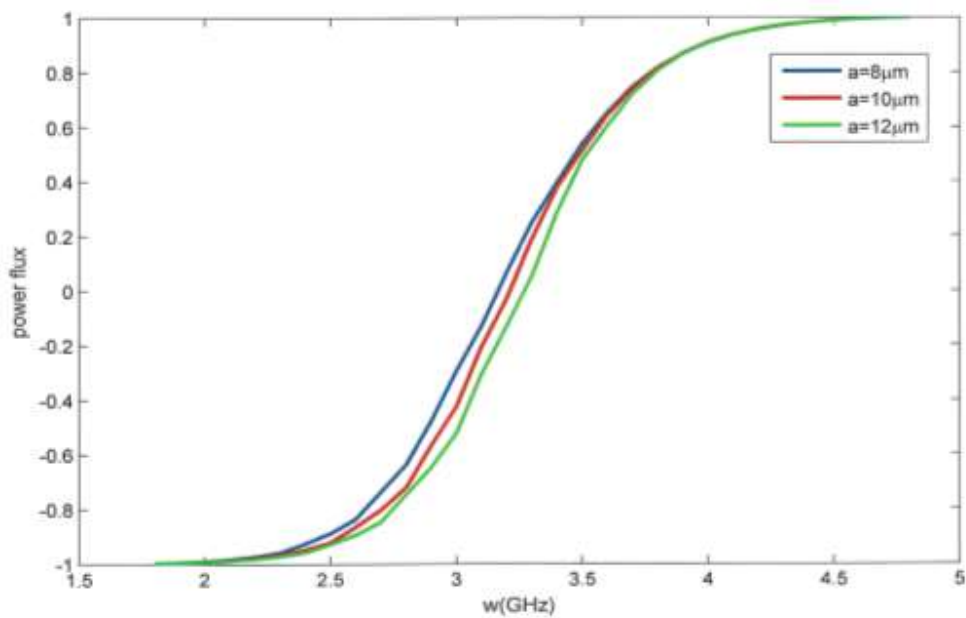


**Fig.(5):** electrical power as a function of frequency  
of  $LP_{01}$  for  $a = (8, 10, 12) \mu m$ .

## 5. CONCLUSION

In this paper, modes in cylindrical waveguide is analysed and it is concluded that modes has frequency dependent permittivity. When the permittivity is between zero and unity . Rigorous *TE* and *TM* modes analysis of cylindrical isotropic metamaterial waveguides has been developed. It was showed that the electromagnetic characteristics of the waveguide are closely dependent on constitutive parameters of the filled metamaterial. The curves of dispersion of the fundamental mode and the first higher-order modes of the metamaterial waveguide are obtained by using Matlab and comparing with COMSOL result. it must be noted here for each mode there is a different propagation way, and the increasing frequency will make propagation forward.

## REFERENCES

- [1] J. B. Pendry, "Negative refraction makes a perfect lens," *Phys. Rev. Lett.*, vol. 85, no. 18, pp. 3966–3969, 2000.
- [2] J. F. Dong and J. Li, "Characteristics of guided modes in uniaxial chiral circular waveguides," *Prog. Electromagn. Res.*, vol. 124, no. January, pp. 331–345, 2012.
- [3] Y. J. Huang, W. T. Lu, and S. Sridhar, "Nanowire waveguide made from extremely anisotropic metamaterials," *Phys. Rev. A - At. Mol. Opt. Phys.*, vol. 77, no. 6, 2008.
- [4] A. N. A. Helal, S. A. Taya, and K. Y. Elwasife, "Propagation of Electromagnetic Waves in Slab Waveguide Structure Consisting of Chiral Nihilty Claddings and Negative-Index Material Core Layer," *Photonic Sensors*, vol. 8, no. 2, pp. 176–187, 2018.
- [5] K. Y. Kim, J.-H. Lee, Y. K. Cho, and H.-S. Tae, "Electromagnetic wave propagation through doubly dispersive subwavelength metamaterial hole," *Opt. Express*, vol. 13, no. 10, p. 3653, 2005.
- [6] M. A. Baqir and P. K. Choudhury, "Flux density through guides with microstructured twisted clad DB medium," *J. Nanomater.*, vol. 2014, no. 2, 2014.
- [7] I. V. Shadrivov, A. A. Sukhorukov, and Y. S. Kivshar, "Guided modes in negative-refractive-index waveguides," *Phys. Rev. E - Stat. Physics, Plasmas, Fluids, Relat. Interdiscip. Top.*, vol. 67, no. 5, p. 4, 2003.
- [8] M. Bertolotti, "Waves in Metamaterials, by L. Solymar and E. Shamonina," *Contemp. Phys.*, vol. 51, no. 6, pp. 545–546, 2010.
- [9] Y. Huang, "Negative refraction in photonic crystals and metamaterials for transformation optics," p. 206, 2011.
- [10] Y. L. Xue, W. Liu, Y. Gu, and Y. Zhang, "Light storage in a cylindrical waveguide with metamaterials," *Opt. Laser Technol.*, vol. 68, no. May 2012, pp. 28–35, 2015.
- [11] M. Tapadas, A. Dissertation, and C. Engineering, "Metamaterials with Negative Permeability and Permittivity : Analysis and Application José Manuel Tapadas Alves Dissertation submitted for obtaining the degree of Master in Electrical and Computer Engineering," *Phy. Rev. Lett.*, vol. 89, pp. 2139021–2139024, 2002.
- [12] X. Tang, B. T. Kuhlmeier, A. Stefani, A. Tuniz, S. C. Fleming, and A. Argyros, "Electromagnetic Wave Propagation Through Air-Core Waveguide with Metamaterial Cladding," *J. Light. Technol.*, vol. 34, no. 22, pp. 5317–5324, 2016.
- [13] M. Beig-Mohammadi, N. Sang-Nourpour, B. C. Sanders, B. R. Lavoie, and R. Kheradmand, "Characterization

of Hybrid Modes in Metamaterial Waveguides,” 2016.

- [14] A. Grbic and G. V. Eleftheriades, “Experimental verification of backward-wave radiation from a negative refractive index metamaterial,” *J. Appl. Phys.*, vol. 92, no. 10, pp. 5930–5935, 2002.
- [15] N. Enghetal, A. Erentok, R. W. Ziolkowski, and A. Am, “Low-index Metamaterials and their Electromagnetic Applications,” *Radio Sci.*, vol. 49, no. 1, pp. 23–36, 2007.
- [16] B. Ghosh and A. B. Kakade, “Guided modes in a metamaterial-filled circular waveguide,” *Electromagnetics*, vol. 32, no. 8, pp. 465–480, 2012.
- [17] G. D’Aguanno, N. Mattiucci, M. Scalora, and M. J. Bloemer, “TE and TM guided modes in an air waveguide with negative-index-material cladding,” *Phys. Rev. E - Stat. Nonlinear, Soft Matter Phys.*, vol. 71, no. 4, pp. 1–7, 2005.
- [18] S. A. Ramakrishna and T. M. Grzegorzcyk, *Physics and applications of negative refractive index materials*. 2008.
- [19] S. T. Ghafel, A. K. Mahdi Salih, and H. A. Yasser, “Theoretical analysis of modes in isotropic metamaterials cylindrical waveguide,” *AIP Conf. Proc.*, vol. 2207, no. February, 2020.